

# On Sparse Regression LDPC Codes

Jamison R. Ebert, Jean-Francois Chamberland, Krishna R. Narayanan  
Department of Electrical and Computer Engineering, Texas A&M University

**Abstract**—Belief propagation applied to iterative decoding and sparse recovery through approximate message passing (AMP) are two research areas that have seen monumental progress in recent decades. Inspired by these advances, this article introduces sparse regression LDPC codes and their decoding. Sparse regression codes (SPARCs) are a class of error correcting codes that build on ideas from compressed sensing and can be decoded using AMP. In certain settings, SPARCs are known to achieve capacity; yet, their performance suffers at finite block lengths. Likewise, LDPC codes can be decoded efficiently using belief propagation and can also be capacity achieving. This article introduces a novel concatenated coding structure that combines an LDPC outer code with a SPARC-inspired inner code. Efficient decoding for such a code can be achieved using AMP with a denoiser that performs belief propagation on the factor graph of the outer LDPC code. The proposed framework exhibits performance improvements over SPARCs and standard LDPC codes for finite block lengths and results in a steep waterfall in error performance, a phenomenon not observed in uncoded SPARCs. Findings are supported by numerical results.

**Index Terms**—LDPC codes, sparse regression codes, approximate message passing, belief propagation.

## I. INTRODUCTION AND BACKGROUND

Low-density parity check (LDPC) codes have been the subject of many scientific inquiries in the past, with landmark contributions ranging from theoretical advances to practical implementations [1]–[8]. LDPC ensembles are amenable to analysis and, under certain conditions, encoded messages can be recovered efficiently using iterative belief propagation (BP) decoding. Interestingly, the complexity of BP decoding grows linearly with block length and, as such, this paradigm offers a pragmatic solution for long block lengths [9]. Some spatially coupled LDPC constructions feature capacity approaching iterative decoding thresholds while also avoiding the pitfall of error floors [10]–[15]. Unfortunately, systems operating at shorter block lengths may not be conducive to the application of spatial coupling. In such situations, non-binary LDPC codes have been leveraged as a means to provide adequate performance [6], [7], [16]–[18].

In a seemingly unrelated research direction, Joseph and Barron introduced the concept of a sparse regression code (SPARC), which establishes a connection between code design and sparse recovery in high dimensions [19]–[21]. The codewords contained in a SPARC codebook consist of sparse superpositions of columns from a design matrix, also known as a sensing matrix in the compressed sensing (CS) literature [22], [23]. In some sense, the SPARC decoding process is equivalent

to recovering the non-zero entries in a suitably designed index vector. Low complexity algorithms have been proposed for the efficient decoding of SPARC codewords. Notably, Rush *et al.* discuss an approximate message passing (AMP) decoder for SPARCs in [24], [25]. It is also worth mentioning that AMP has independently gained much research momentum in recent years owing to its low implementation cost, mathematical tractability, and excellent performance [26]–[30]. Sparse regression codes paired with AMP decoding are known to achieve asymptotic single-user AWGN channel capacity under an appropriately chosen power allocation. Concurrently, there have been efforts to improve the finite block-length performance of SPARCs [31], [32].

A popular strategy to improve the performance of codes in practical settings is to adopt a concatenated structure. For example, SPARCs and LDPC codes have been paired in the past to create concatenated schemes that improve performance [31]–[34]. Concatenated structures with a SPARC-like inner code have also been proposed in unsourced random access [35]–[37]. In [36], it is shown that the structure of a judiciously designed outer code can be integrated into the denoising function of the inner AMP recovery algorithm. Surprisingly, despite being mentioned by Liu *et al.* in [34] as a possible future research direction, such an approach has not been considered for the single-user scenario. This article seeks to address this deficiency by introducing sparse regression LDPC codes.

Sparse regression LDPC codes feature a concatenated inner SPARC-like code and an outer non-binary LDPC code. This concatenated structure is amenable to a decoder that exchanges information between inner and outer codes via a dynamic AMP denoiser. In this setting, the denoiser performs BP on the factor graph of the outer LDPC code to improve the AMP state estimates. This in turn improves the effective observations which in turn translate into better local belief vectors for the BP LDPC decoder. Such a denoiser improves AMP’s convergence and lowers the residual mean square error (MSE) in the estimated SPARC codeword. Once the MSE of the iterative AMP-BP decoding levels off, the outer LDPC code can be leveraged once more to further improve performance. The goal is to use AMP-BP decoding to increase the SNR of the effective observation to a level that exceeds the BP threshold of the graph and then to apply message passing to the outer LDPC code to recover the message. Numerical results demonstrate the performance advantages of the proposed model over related architectures at reasonably short block lengths.

This material is based upon work supported, in part, by the National Science Foundation (NSF) under Grant CCF-2131106, and by Qualcomm Technologies, Inc., through their University Relations Program.

## II. SYSTEM MODEL

We consider a point-to-point memoryless additive white Gaussian noise (AWGN) channel with one transmitter and one receiver, each equipped with a single antenna. The received signal  $\mathbf{y} \in \mathbb{R}^n$  is given by

$$\mathbf{y} = \mathbf{x} + \mathbf{z}, \quad (1)$$

where  $\mathbf{x} \in \mathbb{R}^n$  denotes the transmitted signal and  $\mathbf{z} \sim \mathcal{N}(0, \sigma^2 \mathbf{I})$  represents AWGN. As mentioned above, we wish to study a coding architecture composed of a sparse regression inner code [19]–[21], and a non-binary LDPC outer code [6]–[8]. We elaborate on the encoding process and the decoding scheme below.

### A. Sparse Regression LDPC Encoding

The proposed encoding process features a sequence of three distinct steps:  $q$ -ary LDPC encoding, indexing LDPC symbols, and inner CS encoding. First, the information bits are encoded into a  $q$ -ary LDPC codeword via well-established operations [6]–[8]. The second step transforms the  $q$ -ary LDPC codeword into a suitable sparse vector. The last step is the matrix multiplication emblematic of a sparse regression code; the output is sometimes referred to as a large random matrix system [19]–[21], [34]. We summarize the notions pertaining to this encoding process below while concurrently introducing necessary notation.

1) *q-ary LDPC Encoding*: The LDPC encoder takes a binary sequence  $\mathbf{w} \in \mathbb{F}_2^B$  as its input and maps it to a  $q$ -ary codeword  $\mathbf{v} \in \mathbb{F}_q^L$ . We represent the resultant codeword in concatenated form as

$$\mathbf{v} = (v_1, v_2, \dots, v_L) \quad (2)$$

where the  $\ell$ th element  $v_\ell$  lies in finite field  $\mathbb{F}_q$  and  $L$  is the length of the codeword.

Note that there exists a bijection  $\Phi : \mathbb{F}_q \rightarrow [q]$  between the elements of  $\mathbb{F}_q$  and the integers  $[q] = (0, 1, \dots, q-1)$ , where  $0 \in \mathbb{Z}$  maps to  $0 \in \mathbb{F}_q$  and  $1 \in \mathbb{Z}$  maps to  $1 \in \mathbb{F}_q$ . Throughout, we adopt such an arbitrary, but fixed bijection and exploit this relation by employing the same variable for a field element  $g \in \mathbb{F}_q$  and for its corresponding integer  $\Phi(g) \in [q]$ . This slight abuse of notation greatly simplifies exposition, and its use should not lead to confusion because one can unambiguously infer from context whether an instance refers to the field element or to its integer representation.

2) *LDPC Symbol Indexing*: Coded symbol sparsification/indexing consists of mapping  $v_\ell \in \mathbb{F}_q$  to standard basis vector  $\mathbf{e}_{v_\ell} \in \mathbb{R}^q$  and subsequently stacking the  $L$  basis vectors together. We seize this opportunity to reinforce the notion that entry  $\ell$  of  $\mathbf{v}$  is an element of  $\mathbb{F}_q$ , but  $v_\ell$  in  $\mathbf{e}_{v_\ell}$  refers to an integer in  $[q]$  under our overloaded notation. With that, the output of the indexing process becomes

$$\mathbf{s} = \begin{bmatrix} \mathbf{e}_{v_1} \\ \vdots \\ \mathbf{e}_{v_L} \end{bmatrix}, \quad (3)$$

where  $\mathbf{s}$  is an  $L$ -sparse vector of length  $qL$ . Vector  $\mathbf{s}$  has a structure akin to that of a sparse regression code prior to multiplication by a large random matrix. This structured sparsity can be exploited during decoding.

3) *Inner CS Encoding*: The last phase of the encoding process consists in pre-multiplying vector  $\mathbf{s}$  by matrix  $\mathbf{A}$  to get  $\mathbf{x} = \mathbf{A}\mathbf{s}$ , where  $\mathbf{A} \in \mathbb{R}^{n \times qL}$  and  $\mathbf{A}_{i,j} \sim \mathcal{N}(0, \frac{1}{n})$ . Note that  $n \ll qL$  to conform to the CS framework. Equation (1) may thus be rewritten as:

$$\mathbf{y} = \mathbf{A}\mathbf{s} + \mathbf{z}. \quad (4)$$

Having specified the code structure, we are now ready to discuss the process of recovering  $\mathbf{s}$  from  $\mathbf{y}$ .

### B. Sparse Regression LDPC Decoding

Paralleling the development of AMP for sparse regression codes [24] and drawing inspiration from concatenated AMP systems [33], [34], we wish to create a composite iterative process to recover state vector  $\mathbf{s}$  from  $\mathbf{y}$  that exploits the sparsity in  $\mathbf{s}$  and the parity structure of the LDPC code. This can be accomplished by incorporating message passing on the factor graph of the LDPC code into the AMP denoiser. A similar approach can be found in [36]; however, the denoiser we wish to utilize below differs in the fact that only one codeword is present within  $\mathbf{y}$ .

Our AMP composite algorithm is as follows,

$$\mathbf{r}^{(t)} = \mathbf{A}^T \mathbf{z}^{(t)} + \mathbf{s}^{(t)} \quad (5)$$

$$\mathbf{z}^{(t)} = \mathbf{y} - \mathbf{A}\mathbf{s}^{(t)} + \frac{\mathbf{z}^{(t-1)}}{n} \operatorname{div} \boldsymbol{\eta}_{t-1}(\mathbf{r}^{(t-1)}) \quad (6)$$

$$\mathbf{s}^{(t+1)} = \boldsymbol{\eta}_t(\mathbf{r}^{(t)}) \quad (7)$$

where the superscript  $t$  denotes the iteration count. The algorithm is initialized with conditions  $\mathbf{r}^{(0)} = \mathbf{s}^{(0)} = \mathbf{0}$  and  $\mathbf{z}^{(0)} = \mathbf{y}$ .

Equation (5) specifies the *effective observation*, which is characteristic of AMP. Equation (6) computes the *residual* error enhanced with an Onsager correction term, whereas (7) provides a *state estimate*. The denoising functions  $(\boldsymbol{\eta}_t(\cdot))_{t \geq 0}$  seek to exploit the structure of  $\mathbf{s}$  while computing the state updates.

Generally speaking, a choice denoiser is the conditional expectation of  $\mathbf{s}$  given  $\mathbf{r}^{(t)}$ . Unfortunately, this approach is computationally intractable in the present context because it entails summing over all the possible codewords. As an alternative, we know that BP can be efficiently applied to  $q$ -ary LDPC codes. Furthermore, at any point during BP, a belief on individual LDPC symbols can be formed based on incoming messages from neighboring factor nodes and local observations. Thus, we can potentially apply a few iterations of BP as a means to get an estimate for the state vector by leveraging the connection between sections of  $\mathbf{s}$  and LDPC symbols. In this sense, iterative message passing can act as a foundation for pragmatic denoising functions. We elaborate on this connection below and, concurrently, we review pertinent notions of BP applied to  $q$ -ary LDPC codes.

### III. CREATING A BP DENOISER FOR AMP

In this section, we introduce the denoising function we wish to employ within AMP. To begin, we emphasize that  $\mathbf{r}$  admits a sectionized representation akin to that of the state vector  $\mathbf{s}$  in (3). That is, we can view both the state estimate and the effective observation as concatenations of  $L$  vectors, each of length  $q$ . Mathematically, we have

$$\mathbf{r} = \begin{bmatrix} \mathbf{r}_1 \\ \vdots \\ \mathbf{r}_L \end{bmatrix} \quad \hat{\mathbf{s}} = \begin{bmatrix} \hat{\mathbf{s}}_1 \\ \vdots \\ \hat{\mathbf{s}}_L \end{bmatrix}.$$

This point is crucially important because the denoiser is constructed in a block-wise fashion. As a side note, we neglect the superscript ( $t$ ) for most of the discussion below to lighten notation. Furthermore, we emphasize that the presence of the hat in  $\hat{\mathbf{s}}$  distinguishes the estimate from the true state vector  $\mathbf{s}$  in the absence of an iteration count ( $t$ ).

Each section  $\mathbf{r}_\ell$  in  $\mathbf{r}$  acts as a vector observation about the value of  $\mathbf{s}_\ell \in \{\mathbf{e}_g : g \in [q]\}$ . An astounding and enabling property of AMP is that, under certain technical conditions, the effective observation  $\mathbf{r}$  is asymptotically distributed as  $\mathbf{s} + \tau\boldsymbol{\zeta}$ , where  $\boldsymbol{\zeta}$  is a random vector with independent  $\mathcal{N}(0, 1)$  components and  $\tau$  is a deterministic quantity. This fact hinges on the presence of the Onsager term in (6) and on some smoothness conditions for the denoising functions. We delay the treatment of these technical conditions for the time being; rather, we posit the requirements and formally introduce them as a condition.

**Condition 1.** *The effective observation  $\mathbf{r}^{(t)}$  is asymptotically distributed as  $\mathbf{s} + \tau_t\boldsymbol{\zeta}_t$ , where  $\boldsymbol{\zeta}_t$  is a random vector with independent  $\mathcal{N}(0, 1)$  components and  $\tau_t$  is specified by a set of deterministic equations. This asymptotic characterization takes place in the dimensions of the system, as opposed to time or iteration count.*

We describe below our rationale behind the denoising function assuming Condition 1 holds; we provide a rigorous foundation for this condition in Appendix B, but this can only be done once the structure of the denoiser is established. Consider the effective observation restricted to section  $\ell$ . Under Condition 1, the distribution of random observation vector  $\mathbf{R}_\ell$  given section  $\mathbf{S}_\ell = \mathbf{e}_g$  is given by

$$f_{\mathbf{R}_\ell|\mathbf{S}_\ell}(\mathbf{r}_\ell|\mathbf{e}_g) = \frac{1}{(2\pi)^{\frac{q}{2}}\tau^q} \exp\left(-\frac{\|\mathbf{r}_\ell - \mathbf{e}_g\|^2}{2\tau^2}\right).$$

Under a uniform input distribution, the conditional probability of  $\mathbf{S}_\ell = \mathbf{e}_g$  becomes

$$\begin{aligned} \alpha_\ell(g) &= \Pr(\mathbf{S}_\ell = \mathbf{e}_g|\mathbf{R}_\ell = \mathbf{r}_\ell) = \Pr(V_\ell = g|\mathbf{R}_\ell = \mathbf{r}_\ell) \\ &= \frac{f_{\mathbf{R}_\ell|V_\ell}(\mathbf{r}_\ell|g)}{\sum_{h \in \mathbb{F}_q} f_{\mathbf{R}_\ell|V_\ell}(\mathbf{r}_\ell|h)} = \frac{e^{-\frac{\|\mathbf{r}_\ell - \mathbf{e}_g\|^2}{2\tau^2}}}{\sum_{h \in \mathbb{F}_q} e^{-\frac{\|\mathbf{r}_\ell - \mathbf{e}_h\|^2}{2\tau^2}}} \quad (8) \\ &= \frac{e^{-\frac{r_\ell(g)}{\tau^2}}}{\sum_{h \in \mathbb{F}_q} e^{-\frac{r_\ell(h)}{\tau^2}}}. \end{aligned}$$

A possible estimate for  $\mathbf{S}_\ell$  can be computed by taking its conditional expectation, given observation  $\mathbf{R}_\ell = \mathbf{r}_\ell$ , with

$$\mathbb{E}[\mathbf{S}_\ell|\mathbf{R}_\ell = \mathbf{r}_\ell] = \sum_{g \in \mathbb{F}_q} \mathbf{e}_g \Pr(\mathbf{S}_\ell = \mathbf{e}_g|\mathbf{R}_\ell = \mathbf{r}_\ell). \quad (9)$$

A variant of this approach can be found in [24] for a system without an outer code. Ideally, we would like to take advantage of the outer code with the more precise MMSE estimate of the form  $\mathbb{E}[\mathbf{S}_\ell|\mathbf{R} = \mathbf{r}]$ . Unfortunately, as mentioned above, computing this conditional expectation is far too complex to be implemented in practice. A viable alternative that trades off performance and complexity is to execute BP on the factor graph of the outer LDPC code. Implicitly, this approach computes an estimate for every  $\mathbf{S}_\ell$  based on the computation tree of the code, up to a certain depth [8], [38].

Frameworks to perform BP on factor graphs are well-established [39]; thus, we assume some familiarity with such iterative procedures. We proceed by first considering the nuances of non-binary LDPC factor graphs, then presenting a BP algorithm, and finally proposing a dynamic denoiser for SR-LDPC codes.

#### A. Non-Binary LDPC Graphs

The factor graph for an  $\mathbb{F}_q$  LDPC code features  $L$  variable (left) nodes and  $L(1 - R)$  check (right) nodes enforcing parity constraints, where  $R$  is the *rate* of the LDPC code [6]–[8]. An important distinction between binary and non-binary LDPC codes is that a factor graph for the latter code typically includes edge labels. These labels take values in  $\mathbb{F}_q \setminus \{0\}$ . A vector  $\mathbf{v} \in \mathbb{F}_q^L$  is a valid codeword if it satisfies the parity equations

$$\sum_{v_\ell \in N(c_p)} \omega_{\ell,p} \otimes v_\ell = 0 \quad \forall p \in [L(1 - R)], \quad (10)$$

where  $N(c_p)$  is the collection of variable nodes adjacent to parity check  $c_p$ . The summation and the multiplication operator  $\otimes$  in (10) take place over finite field  $\mathbb{F}_q$ . Parameter  $\omega_{\ell,p}$  represents the label or weight assigned with the edge connecting variable node  $v_\ell$  and check node  $c_p$ . Adopting common factor graph concepts [39], [40], we denote the graph neighbors of variable node  $v_\ell$  by  $N(v_\ell)$ . The factor associated with  $c_p$  and derived from parity equation (10) can be expressed as an indicator function

$$\mathcal{G}_p(\mathbf{v}_p) = \mathbf{1} \left( \sum_{v_\ell \in N(c_p)} \omega_{\ell,p} \otimes v_\ell = 0 \right) \quad (11)$$

where  $\mathbf{v}_p = (v_\ell \in N(c_p))$  is a shorthand notation for the restriction of  $\mathbf{v}$  to entries associated with graph neighborhood  $N(c_p)$ . With these definitions, the factor function associated with our LDPC code assumes the product decomposition given by

$$\mathcal{G}(\mathbf{v}) = \prod_{p \in [L(1-R)]} \mathcal{G}_p(\mathbf{v}_p). \quad (12)$$

In words,  $\mathcal{G}(\mathbf{v})$  is an indicator function that assesses whether its argument is a valid codeword.

## B. Belief Propagation

We view messages for a non-binary LDPC code as multi-dimensional belief vectors over  $\mathbb{F}_q$ . Messages from variable nodes to check nodes are denoted by  $\boldsymbol{\mu}_{v \rightarrow c}$ , and messages in the reverse direction are represented by  $\boldsymbol{\mu}_{c \rightarrow v}$ . Formally, a message going from check node  $c_p$  to variable node  $v_\ell \in N(c_p)$  is computed component-wise through

$$\boldsymbol{\mu}_{c_p \rightarrow v_\ell}(g) = \sum_{\mathbf{v}_p: \mathbf{v}_\ell = g} \mathcal{G}_p(\mathbf{v}_p) \prod_{v_j \in N(c_p) \setminus v_\ell} \boldsymbol{\mu}_{v_j \rightarrow c_p}(g_j). \quad (13)$$

While (13) is shown in compact form, the actual summation operation is cumbersome. Finding the set of summands entails identifying sequences of the form  $(g_j \in \mathbb{F}_q : v_j \in N(c_p) \setminus v_\ell)$  that fulfill local condition (10) or, equivalently,

$$\sum_{v_j \in N(c_p) \setminus v_\ell} \omega_{j,p} \otimes g_j = -\omega_{\ell,p} \otimes g. \quad (14)$$

A belief vector passed from variable node  $v_\ell$  to check node  $c_p$ , where  $p \in N(v_\ell)$ , is calculated component-wise via

$$\boldsymbol{\mu}_{v_\ell \rightarrow c_p}(g) \propto \boldsymbol{\alpha}_\ell(g) \prod_{c_\xi \in N(v_\ell) \setminus c_p} \boldsymbol{\mu}_{c_\xi \rightarrow v_\ell}(g). \quad (15)$$

The ‘ $\propto$ ’ symbol indicates that the positive measure can be normalized before being sent out as a message. Vector  $\boldsymbol{\alpha}_\ell$  in (15) can be viewed as a collection of beliefs based on local observations, as in (8). That is, entry  $\alpha_\ell(g)$  captures the probability that symbol  $g$  is the true field element within section  $\ell$ . Other BP messages are initialized with  $\boldsymbol{\mu}_{v \rightarrow c} = \mathbf{1}$  and  $\boldsymbol{\mu}_{c \rightarrow v} = \mathbf{1}$ . The traditional parallel sum-product algorithm iterates between (13) and (15), alternating between updated rightbound messages and leftbound messages.

One of the key advantages of indexing vectors using field elements in  $\mathbb{F}_q$ , as pointed out in [7], is the ensuing ability to define pertinent operators on these vectors. Paralleling established literature, we define two actions.

**Definition 2** (Vector  $+g$  Operator [7]). *For field element  $g \in \mathbb{F}_q$ , the vector  $+g$  operator acting on  $\mathbf{b}$  and denoted by  $\mathbf{b}^{+g}$  is defined as*

$$\begin{aligned} \mathbf{b}^{+g} &= (b_g, b_{g \oplus 1}, \dots, b_{g \oplus (q-1)}) \\ &= (b_{h \oplus g} : h \in \mathbb{F}_q) \end{aligned}$$

where subscript addition  $\oplus$  is performed in  $\mathbb{F}_q$ .

**Definition 3** (Vector  $\times g$  Operator [7]). *For field element  $g \in \mathbb{F}_q \setminus \{0\}$ , we define the vector  $\times g$  operator acting on  $\mathbf{b}$  and denoted by  $\mathbf{b}^{\times g}$  by*

$$\begin{aligned} \mathbf{b}^{\times g} &= (b_0, b_g, b_{2 \otimes g}, \dots, b_{(q-1) \otimes g}) \\ &= (b_{h \otimes g} : h \in \mathbb{F}_q) \end{aligned}$$

where subscript product  $\otimes$  takes place in  $\mathbb{F}_q$ .

Under these operations, we can rewrite (13) in a concise manner:

$$\boldsymbol{\mu}_{c_p \rightarrow v_\ell} = \left( \bigodot_{v_j \in N(c_p) \setminus v_\ell} \left( \boldsymbol{\mu}_{v_j \rightarrow c_p} \right)^{\times \omega_{j,p}^{-1}} \right)^{\times (-\omega_{\ell,p})} \quad (16)$$

where  $\omega_{j,p}$  is the label on the edge between variable node  $v_j$  and factor node  $c_p$ . The operator  $\odot$  denotes the  $\mathbb{F}_q$  convolution between two vectors,

$$[\boldsymbol{\mu} \odot \boldsymbol{\nu}]_g = \sum_{h \in \mathbb{F}_q} \mu_h \cdot \nu_{g-h} \quad g \in \mathbb{F}_q.$$

The exposition can be simplified further if we absorb the edge labels within the messages themselves. Specifically, we adopt the definitions

$$\bar{\boldsymbol{\mu}}_{v_j \rightarrow c_p} = \left( \boldsymbol{\mu}_{v_j \rightarrow c_p} \right)^{\times \omega_{j,p}^{-1}} \quad (17)$$

$$\bar{\boldsymbol{\mu}}_{c_p \rightarrow v_\ell} = \left( \boldsymbol{\mu}_{c_p \rightarrow v_\ell} \right)^{\times (-\omega_{\ell,p}^{-1})}. \quad (18)$$

Then (16) morphs into the simpler expression

$$\bar{\boldsymbol{\mu}}_{c_p \rightarrow v_\ell} = \bigodot_{v_j \in N(c_p) \setminus v_\ell} \bar{\boldsymbol{\mu}}_{v_j \rightarrow c_p}. \quad (19)$$

This equation highlights the role of the  $\mathbb{F}_q$  convolution within BP for non-binary LDPC codes. The message from variable node  $v_\ell$  to check node  $c_p$  found in (15) also admits a more compact form. For  $p \in N(v_\ell)$ , the traditional outgoing message from a variable node can be written as

$$\boldsymbol{\mu}_{v_\ell \rightarrow c_p} = \frac{\boldsymbol{\alpha}_\ell \circ \left( \bigodot_{c_\xi \in N(v_\ell) \setminus c_p} \boldsymbol{\mu}_{c_\xi \rightarrow v_\ell} \right)}{\left\| \boldsymbol{\alpha}_\ell \circ \left( \bigodot_{c_\xi \in N(v_\ell) \setminus c_p} \boldsymbol{\mu}_{c_\xi \rightarrow v_\ell} \right) \right\|_1} \quad (20)$$

where  $\circ$  represents the Hadamard product.

A natural estimate for the distribution associated with variable node  $v_\ell$ , including intrinsic information, is

$$\hat{\mathbf{S}}_\ell = \frac{\boldsymbol{\alpha}_\ell \circ \left( \bigodot_{c_p \in N(v_\ell)} \boldsymbol{\mu}_{c_p \rightarrow v_\ell} \right)}{\left\| \boldsymbol{\alpha}_\ell \circ \left( \bigodot_{c_p \in N(v_\ell)} \boldsymbol{\mu}_{c_p \rightarrow v_\ell} \right) \right\|_1}. \quad (21)$$

As we will shortly see, (21) is the output of our proposed denoiser.

**Remark 4.** *In our construction,  $q = 2^m, m \geq 1$  because indexing is derived from sequences of bits. This invites the application of fast techniques to implement message passing over the corresponding factor graph. Specifically, the fast Walsh-Hadamard transform (FWHT) can be utilized to rapidly and efficiently compute (19), with*

$$\bar{\boldsymbol{\mu}}_{c_p \rightarrow v_\ell} \propto \text{fwht}^{-1} \left( \prod_{v_j \in N(c_p) \setminus v_\ell} \text{fwht} \left( \bar{\boldsymbol{\mu}}_{v_j \rightarrow c_p} \right) \right).$$

Alternatively, one could adopt a different finite field convolution or a ring structure amenable to the circular convolution to create local factor functions conducive to the fast Fourier transform [6], [41], [42].

With these tools in mind, we are ready to formally define our proposed denoiser.

### C. Sparse Regression LDPC Denoiser

Conceptually, one can initiate the state of the LDPC factor graph using the effective observation  $\mathbf{r}$ , run BP, and then gain an estimate for the state based on (21). As mentioned before, in the absence of BP iterations, local estimates reduce to the conditional expectation  $\mathbb{E}[\mathbf{S}_\ell | \mathbf{R}_\ell = \mathbf{r}_\ell]$  found in (9). Yet, as more iterations of the BP algorithm are performed, the estimate for  $\mathbf{S}_\ell$  is refined based on the computation tree of the outer code, up to a certain depth.

**Definition 5** (BP-N Denoiser). *Let  $N$  denote the number of BP iterations to perform, where  $N$  is less than the girth of the LDPC factor graph. The BP-N denoiser*

- 1) *initializes the LDPC factor graph with estimates  $\alpha_\ell$  computed from  $\mathbf{r}_\ell$  for  $\ell \in [L]$  according to (8);*
- 2) *computes and passes variable to check messages (see (20)) and check to variable messages (see (17), (19), (18) and Remark 4) along the edges of the factor graph in an alternating fashion  $N$  times;*
- 3) *computes updated state estimates according to (21).*

*The output of this denoiser can then be passed to the AMP composite algorithm for the computation of the next residual, enhanced with the Onsager term.*

The derivation of the Onsager correction term corresponding to this denoiser is included in Appendix A. At this point, we turn to a performance assessment of sparse regression LDPC codes via numerical simulations.

## IV. SIMULATION RESULTS

In this section, we seek to characterize the performance of SR-LDPC codes.<sup>1</sup> As benchmarks, we compare our results to the concatenated SPARC/LDPC scheme presented in [31] as well as 5G-NR binary LDPC encoded BPSK. We note that the latter comparison provides limited insight because the SR-LDPC code is allowed real channel inputs whereas the 5G-NR code is constrained to binary inputs; nevertheless, we make the comparison to see whether SR-LDPC codes are competitive with state of the art, commonly used codes.

The scenario of interest is one in which 5888 information bits are to be transmitted over 7350 real channel uses. We define the SR-LDPC rate to be the number of information bits over the number of channel uses; thus, we have that  $R_{\text{SR-LDPC}} \approx 0.80$ . The non-binary LDPC code employed is a (751, 736) code ( $R_{\text{LDPC}} \approx 0.98$ ) over  $\text{GF}(256)$  whose edges are generated via progressive edge growth (PEG) and whose weights were chosen uniformly at random from the elements of  $\mathbb{F}_{256} \setminus 0$ . The fraction of degree-2 variable nodes is chosen to be higher than usual so that the AMP-BP iterations can bootstrap in high-noise environments. The AMP-BP decoder is run for up to 100 iterations and then the non-binary LDPC BP decoder is run for another 100 iterations, or until a valid codeword is obtained. Figure 1 highlights our results.

<sup>1</sup>The source code used to generate these results is available online at <https://github.com/EngProjects/mMTC/tree/code>.

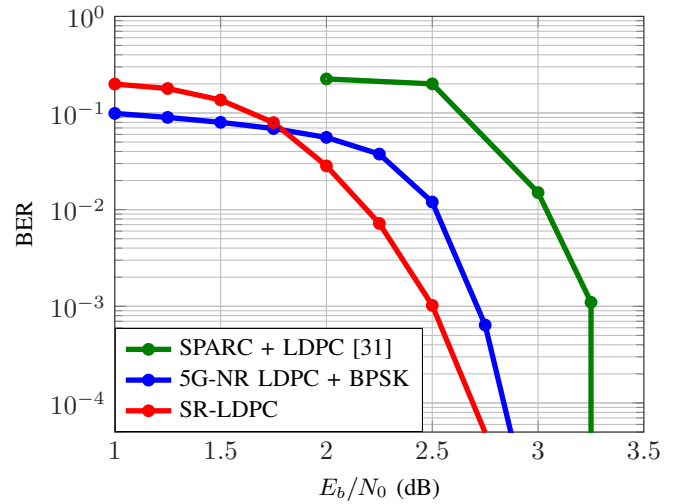


Fig. 1: BER performance comparison of a sparse regression LDPC code, the concatenated SPARC/LDPC construction from [31], and 5G-NR binary LDPC encoded BPSK as a function of  $E_b/N_0$ . The SR-LDPC code requires a lower  $E_b/N_0$  to achieve a target BER than LDPC encoded BPSK and the scheme in [31].

From Fig. 1, it is clear that sparse regression LDPC codes provide a roughly 0.75 dB improvement at a BER of  $10^{-3}$  over other SPARC/LDPC concatenated coding structures. Furthermore, the SR-LDPC code outperforms 5G-NR LDPC encoded BPSK in some regimes; we note however, that 5G-NR LDPC encoded BPSK has a lower error floor than the SR-LDPC code.

## V. CONCLUSION

In conclusion, this article presents sparse regression LDPC codes and their decoding. A sparse regression code is a concatenated structure with an inner SPARC-like code and an outer non-binary LDPC code. The inner code is decoded using AMP with a dynamic denoiser which runs BP on the factor graph of the outer LDPC code to improve the state estimate at every iteration. After running many iterations of the AMP-BP decoder, the final effective observation is fed into a standard LDPC BP decoder, which seeks to correct any residual errors that may be present in the received signal. Numerical results show that sparse regression codes exhibit performance improvements over standard LDPC codes and other concatenated SPARC/LDPC constructions.

As mentioned in the introduction, both SPARCs and LDPC codes are known to achieve capacity in certain circumstances, yet both codes generally suffer at short block lengths. The success of sparse regression LDPC codes is evidence that SPARCs and LDPC codes can be seamlessly combined to significantly improve performance. Directions for future work include optimizing the outer LDPC code and applying coded demixing [37] to SR-LDPC codes to accommodate multiple users.

## REFERENCES

- [1] R. Gallager, "Low-density parity-check codes," *IEEE Trans. Inform. Theory*, vol. 8, no. 1, pp. 21–28, 1962.
- [2] D. J. C. MacKay, "Good error-correcting codes based on very sparse matrices," *IEEE Trans. Inform. Theory*, vol. 45, no. 2, pp. 399–431, 1999.
- [3] M. G. Luby, M. Mitzenmacher, M. A. Shokrollahi, and D. A. Spielman, "Improved low-density parity-check codes using irregular graphs," *IEEE Trans. Inform. Theory*, vol. 47, no. 2, pp. 585–598, 2001.
- [4] T. J. Richardson and R. L. Urbanke, "The capacity of low-density parity-check codes under message-passing decoding," *IEEE Trans. Inform. Theory*, vol. 47, no. 2, pp. 599–618, 2001.
- [5] S.-Y. Chung, T. J. Richardson, and R. L. Urbanke, "Analysis of sum-product decoding of low-density parity-check codes using a gaussian approximation," *IEEE Trans. Inform. Theory*, vol. 47, no. 2, pp. 657–670, 2001.
- [6] M. C. Davey and D. J. C. MacKay, "Low density parity check codes over  $GF(q)$ ," in *Information Theory Workshop*. IEEE, 1998, pp. 70–71.
- [7] A. Bannatan and D. Burshtein, "Design and analysis of nonbinary LDPC codes for arbitrary discrete-memoryless channels," *IEEE Trans. Inform. Theory*, vol. 52, no. 2, pp. 549–583, 2006.
- [8] T. J. Richardson and R. L. Urbanke, *Modern coding theory*, Cambridge University Press, 2008.
- [9] D. J. Costello, L. Dolecek, T. E. Fuja, J. Kliewer, D. G. M. Mitchell, and R. Smarandache, "Spatially coupled sparse codes on graphs: Theory and practice," *IEEE Communications Magazine*, vol. 52, no. 7, pp. 168–176, 2014.
- [10] A. J. Felstrom and K. Sh. Zigangirov, "Time-varying periodic convolutional codes with low-density parity-check matrix," *IEEE Trans. Inform. Theory*, vol. 45, no. 6, pp. 2181–2191, 1999.
- [11] M. Lentmaier, A. Sridharan, D. J. Costello, and K. Sh. Zigangirov, "Iterative decoding threshold analysis for LDPC convolutional codes," *IEEE Trans. Inform. Theory*, vol. 56, no. 10, pp. 5274–5289, 2010.
- [12] S. Kudekar, T. J. Richardson, and R. L. Urbanke, "Spatially coupled ensembles universally achieve capacity under belief propagation," *IEEE Trans. Inform. Theory*, vol. 59, no. 12, pp. 7761–7813, 2013.
- [13] A. Yedla, Y.-Y. Jian, P. S. Nguyen, and H. D. Pfister, "A simple proof of maxwell saturation for coupled scalar recursions," *IEEE Trans. Inform. Theory*, vol. 60, no. 11, pp. 6943–6965, 2014.
- [14] S. Kumar, A. J. Young, N. Macris, and H. D. Pfister, "Threshold saturation for spatially coupled LDPC and LDGM codes on BMS channels," *IEEE Trans. Inform. Theory*, vol. 60, no. 12, pp. 7389–7415, 2014.
- [15] I. Andriyanova and A. Graell i Amat, "Threshold saturation for nonbinary SC-LDPC codes on the binary erasure channel," *IEEE Trans. Inform. Theory*, vol. 62, no. 5, pp. 2622–2638, 2016.
- [16] D. Declercq and M. Fossorier, "Decoding algorithms for nonbinary ldpc codes over  $gf(q)$ ," *IEEE Trans. on Commun.*, vol. 55, no. 4, pp. 633–643, 2007.
- [17] A. Voicila, D. Declercq, F. Verdier, M. Fossorier, and P. Urard, "Low-complexity decoding for non-binary LDPC codes in high order fields," *IEEE Trans. on Commun.*, vol. 58, no. 5, pp. 1365–1375, 2010.
- [18] B.-Y. Chang, D. Divsalar, and L. Dolecek, "Non-binary protograph-based LDPC codes for short block-lengths," in *Information Theory Workshop*. IEEE, 2012, pp. 282–286.
- [19] A. Joseph and A. R. Barron, "Least squares superposition codes of moderate dictionary size are reliable at rates up to capacity," *IEEE Trans. Inform. Theory*, vol. 58, no. 5, pp. 2541–2557, 2012.
- [20] A. Joseph and A. R. Barron, "Fast sparse superposition codes have near exponential error probability for  $R < C$ ," *IEEE Trans. Inform. Theory*, vol. 60, no. 2, pp. 919–942, 2013.
- [21] R. Venkataramanan, S. Tatikonda, and A. Barron, "Sparse regression codes," *Foundations and Trends in Communications and Information Theory*, vol. 15, no. 1–2, pp. 1–195, 2019.
- [22] D. L. Donoho, "Compressed sensing," *IEEE Trans. Inform. Theory*, vol. 52, no. 4, pp. 1289–1306, 2006.
- [23] E. J. Candès, J. Romberg, and T. Tao, "Robust uncertainty principles: Exact signal reconstruction from highly incomplete frequency information," *IEEE Trans. Inform. Theory*, vol. 52, no. 2, pp. 489–509, 2006.
- [24] C. Rush, A. Greig, and R. Venkataramanan, "Capacity-achieving sparse superposition codes via approximate message passing decoding," *IEEE Trans. Inform. Theory*, vol. 63, no. 3, pp. 1476–1500, 2017.
- [25] C. Rush, K. Hsieh, and R. Venkataramanan, "Capacity-achieving spatially coupled sparse superposition codes with AMP decoding," *IEEE Trans. Inform. Theory*, vol. 67, no. 7, pp. 4446–4484, 2021.
- [26] D. L. Donoho, A. Maleki, and A. Montanari, "Message-passing algorithms for compressed sensing," *Proc. National Academy of Sciences*, vol. 106, no. 45, pp. 18914–18919, 2009.
- [27] M. Bayati and A. Montanari, "The dynamics of message passing on dense graphs, with applications to compressed sensing," *IEEE Trans. Inform. Theory*, vol. 57, no. 2, pp. 764–785, 2011.
- [28] A. Javanmard and A. Montanari, "State evolution for general approximate message passing algorithms, with applications to spatial coupling," *IMA Information and Inference*, vol. 2, no. 2, pp. 115–144, 2013.
- [29] M. Bayati, M. Lelarge, and A. Montanari, "Universality in polytope phase transitions and message passing algorithms," *The Annals of Applied Probability*, vol. 25, no. 2, pp. 753–822, 2015.
- [30] R. Berthier, A. Montanari, and P.-M. Nguyen, "State evolution for approximate message passing with non-separable functions," *IMA Information and Inference*, vol. 9, no. 1, pp. 33–79, 2020.
- [31] A. Greig and R. Venkataramanan, "Techniques for improving the finite length performance of sparse superposition codes," *IEEE Trans. on Commun.*, vol. 66, no. 3, pp. 905–917, 2017.
- [32] H. Cao and P. O. Vontobel, "Using list decoding to improve the finite-length performance of sparse regression codes," *IEEE Trans. on Commun.*, vol. 69, no. 7, pp. 4282–4293, 2021.
- [33] S. Liang, C. Liang, J. Ma, and L. Ping, "Compressed coding, AMP-based decoding, and analog spatial coupling," *IEEE Trans. on Commun.*, vol. 68, no. 12, pp. 7362–7375, 2020.
- [34] L. Liu, C. Liang, J. Ma, and L. Ping, "Capacity optimality of AMP in coded systems," *IEEE Trans. Inform. Theory*, vol. 67, no. 7, pp. 4429–4445, 2021.
- [35] A. Fengler, P. Jung, and G. Caire, "SPARCs for unsourced random access," *IEEE Trans. Inform. Theory*, vol. 67, no. 10, pp. 6894–6915, 2021.
- [36] V. K. Amalladinne, A. K. Pradhan, C. Rush, J.-F. Chamberland, and K. R. Narayanan, "Unsourced random access with coded compressed sensing: Integrating AMP and belief propagation," *IEEE Trans. Inform. Theory*, vol. 68, no. 4, pp. 2384–2409, 2022.
- [37] J. R. Ebert, V. K. Amalladinne, S. Rini, J.-F. Chamberland, and K. R. Narayanan, "Coded demixing for unsourced random access," *IEEE Trans. Signal Processing*, vol. 70, pp. 2972–2984, 2022.
- [38] N. Wiberg, H.-A. Loeliger, and R. Kotter, "Codes and iterative decoding on general graphs," *European Trans. Telecommunications*, vol. 6, no. 5, pp. 513–525, 1995.
- [39] F. R. Kschischang, B. J. Frey, and H.-A. Loeliger, "Factor graphs and the sum-product algorithm," *IEEE Trans. Inform. Theory*, vol. 47, no. 2, pp. 498–519, 2001.
- [40] H.-A. Loeliger, "An introduction to factor graphs," *IEEE Signal Processing Mag.*, vol. 21, no. 1, pp. 28–41, 2004.
- [41] H. Song and J. R. Cruz, "Reduced-complexity decoding of Q-ary LDPC codes for magnetic recording," *IEEE Trans. on Magnetics*, vol. 39, no. 2, pp. 1081–1087, 2003.
- [42] A. Goupil, M. Colas, G. Gelle, and D. Declercq, "FFT-based BP decoding of general LDPC codes over Abelian groups," *IEEE Trans. on Commun.*, vol. 55, no. 4, pp. 644–649, 2007.

APPENDIX A  
DERIVATION OF ONSAGER TERM

Intuitively, the role of the Onsager term is to (asymptotically) cancel the first-order correlations between  $\mathbf{A}^T \mathbf{z}^{(t)}$  and  $\mathbf{s}^{(t)}$  and thereby maintain a structure conducive to prompt convergence and analysis. This factor, emblematic of AMP algorithms, appears in (6) and is given by

$$\begin{aligned} & \frac{\mathbf{z}^{(t-1)}}{n} \operatorname{div} \boldsymbol{\eta}_{t-1} \left( \mathbf{A}^T \mathbf{z}^{(t-1)} + \mathbf{s}^{(t-1)} \right) \\ &= \frac{\mathbf{z}^{(t-1)}}{n} \operatorname{div} \boldsymbol{\eta}_{t-1} \left( \mathbf{r}^{(t-1)} \right) \end{aligned}$$

where the div operator can be expanded into

$$\operatorname{div} \boldsymbol{\eta}(\mathbf{r}) = \sum_{\ell \in [L]} \operatorname{div} \hat{\mathbf{s}}_{\ell}(\mathbf{r}, \tau) = \sum_{\ell \in [L]} \sum_{g \in \mathbb{F}_q} \frac{\partial \hat{\mathbf{s}}_{\ell}(g, \mathbf{r}, \tau)}{\partial \mathbf{r}_{\ell}(g)}. \quad (22)$$

Thus, as an intermediate step, we must calculate the partial derivative of  $\hat{\mathbf{s}}_{\ell}(g, \mathbf{r}, \tau)$  with respect to  $\mathbf{r}_{\ell}(g)$ . This computation is rendered much simpler under the following condition.

**Condition 6** (Sub-Girth AMP-BP). *The BP-N denoiser is said to possess the sub-girth AMP-BP condition when fewer message passing iterations are performed on the factor graph of the LDPC code than the shortest cycle of this same graph, per AMP denoising step.*

This condition ensures that the message passing operations employed during denoising yield valid computation trees without cycles. Fortunately, this is the regime we are primarily interested in.

**Lemma 7.** *Under Condition 6, the partial derivative of  $\hat{\mathbf{s}}_{\ell}(g, \mathbf{r}, \tau)$  with respect to  $\mathbf{r}_{\ell}(g)$  is equal to*

$$\frac{\partial \hat{\mathbf{s}}_{\ell}(g, \mathbf{r}, \tau)}{\partial \mathbf{r}_{\ell}(g)} = \frac{1}{\tau^2} \hat{\mathbf{s}}_{\ell}(g, \mathbf{r}, \tau) (1 - \hat{\mathbf{s}}_{\ell}(g, \mathbf{r}, \tau)) \quad (23)$$

where  $g \in \mathbb{F}_q$ .

*Proof:* Recall that the output of the BP denoiser defined in (21) can be expressed as

$$\begin{aligned} \hat{\mathbf{s}}_{\ell}(g, \mathbf{r}, \tau) &= \frac{\boldsymbol{\alpha}_{\ell}(g) \prod_{p \in N(v_{\ell})} \boldsymbol{\mu}_{c_p \rightarrow v_{\ell}}(g)}{\sum_{h \in \mathbb{F}_q} \boldsymbol{\alpha}_{\ell}(h) \prod_{p \in N(v_{\ell})} \boldsymbol{\mu}_{c_p \rightarrow v_{\ell}}(h)} \\ &= \frac{\boldsymbol{\alpha}_{\ell}(g) \boldsymbol{\mu}_{v_{\ell} \rightarrow c_0}(g)}{\sum_{h \in \mathbb{F}_q} \boldsymbol{\alpha}_{\ell}(h) \boldsymbol{\mu}_{v_{\ell} \rightarrow c_0}(h)}. \end{aligned} \quad (24)$$

Under Condition 6, belief vector  $\boldsymbol{\mu}_{v_{\ell} \rightarrow c_0}$  is based solely on extrinsic information and, hence, it is determined based on  $\{\mathbf{r}_j : j \in [L] \setminus \{\ell\}\}$ . Consequence, we gather that

$$\frac{\partial \boldsymbol{\mu}_{v_{\ell} \rightarrow c_0}(g)}{\partial \mathbf{r}_{\ell}(g)} = 0.$$

Under such circumstances, we can calculate the desired derivative in a straightforward manner, with

$$\begin{aligned} \frac{\partial \hat{\mathbf{s}}_{\ell}(g, \mathbf{r}, \tau)}{\partial \mathbf{r}_{\ell}(g)} &= \frac{\partial}{\partial \mathbf{r}_{\ell}(g)} \frac{e^{\frac{\mathbf{r}_{\ell}(g)}{\tau^2}} \boldsymbol{\mu}_{v_{\ell} \rightarrow c_0}(g)}{\sum_{h \in \mathbb{F}_q} e^{\frac{\mathbf{r}_{\ell}(h)}{\tau^2}} \boldsymbol{\mu}_{v_{\ell} \rightarrow c_0}(h)} \\ &= \frac{1}{\tau^2} \frac{e^{\frac{\mathbf{r}_{\ell}(g)}{\tau^2}} \boldsymbol{\mu}_{v_{\ell} \rightarrow c_0}(g)}{\sum_{h \in \mathbb{F}_q} e^{\frac{\mathbf{r}_{\ell}(g)}{\tau^2}} \boldsymbol{\mu}_{v_{\ell} \rightarrow c_0}(g)} \\ &\quad - \frac{1}{\tau^2} \frac{\left( e^{\frac{\mathbf{r}_{\ell}(g)}{\tau^2}} \boldsymbol{\mu}_{v_{\ell} \rightarrow c_0}(g) \right)^2}{\left( \sum_{h \in \mathbb{F}_q} e^{\frac{\mathbf{r}_{\ell}(g)}{\tau^2}} \boldsymbol{\mu}_{v_{\ell} \rightarrow c_0}(g) \right)^2} \\ &= \frac{1}{\tau^2} \hat{\mathbf{s}}_{\ell}(g, \mathbf{r}, \tau) (1 - \hat{\mathbf{s}}_{\ell}(g, \mathbf{r}, \tau)). \end{aligned}$$

This last line corresponds to the statement of the lemma. ■

It is worth emphasizing that the derivative in (23) remains unchanged irrespective of the number of BP rounds computed on the factor graph, so long as Condition 6 is satisfied. The divergence of (22) assumes the same simple form under such circumstances.

**Proposition 8.** *The divergence of  $\boldsymbol{\eta}(\mathbf{r})$  with respect to  $\mathbf{r}$  is equal to*

$$\operatorname{div} \boldsymbol{\eta}(\mathbf{r}) = \frac{1}{\tau^2} \left( \|\boldsymbol{\eta}(\mathbf{r})\|_1 - \|\boldsymbol{\eta}(\mathbf{r})\|^2 \right). \quad (25)$$

*Proof:* We expand the div operator as

$$\begin{aligned} \operatorname{div} \boldsymbol{\eta}(\mathbf{r}) &= \sum_{\ell \in [L]} \operatorname{div} \hat{\mathbf{s}}_{\ell}(\mathbf{r}, \tau) = \sum_{\ell \in [L]} \sum_{g \in \mathbb{F}_q} \frac{\partial \hat{\mathbf{s}}_{\ell}(g, \mathbf{r}, \tau)}{\partial \mathbf{r}_{\ell}(g)} \\ &= \sum_{\ell \in [L]} \sum_{g \in \mathbb{F}_q} \frac{1}{\tau^2} \hat{\mathbf{s}}_{\ell}(g, \mathbf{r}, \tau) (1 - \hat{\mathbf{s}}_{\ell}(g, \mathbf{r}, \tau)) \\ &= \frac{1}{\tau^2} \left( \|\boldsymbol{\eta}(\mathbf{r})\|_1 - \|\boldsymbol{\eta}(\mathbf{r})\|^2 \right). \end{aligned} \quad (26)$$

The last equality follows from the fact that, since  $\hat{\mathbf{s}}_{\ell}(g, \mathbf{r}, \tau)$  lies between zero and one, the corresponding partial derivative with respect to  $\mathbf{r}_{\ell}(g)$  found in Lemma 7 is always non-negative. ■

APPENDIX B  
DENOISER IS LIPSCHITZ CONTINUOUS

The mathematical underpinnings for the rigorous application of AMP in this article are presented by Berthier, Montanari, and Nguyen in [30]. One of the conditions for the state evolution to hold for non-separable functions is that the denoiser must be pseudo-Lipschitz of a certain order. For the problem at hand, we are able to show the stronger Lipschitz condition, which is sufficient. Thus, the main objective of this section is to demonstrate that the denoiser introduced in Definition 5 is Lipschitz continuous under Condition 6. To achieve this goal, our strategy is to demonstrate that the magnitudes of the entries in the Jacobian matrix of  $\boldsymbol{\eta}(\mathbf{r})$  with respect to  $\mathbf{r}$  are uniformly bounded.

Recall that the denoiser assumes a sectional form, as described in Definition 5. The vector estimate for section  $\ell$  becomes

$$\hat{\mathbf{s}}_\ell(\mathbf{r}) = \sum_{g \in \mathbb{F}_q} \Pr(V_\ell = g | \mathbf{R}_{\text{tree}} = \mathbf{r}_{\text{tree}}) \mathbf{e}_g,$$

where  $\mathbf{R}_{\text{tree}}$  denotes the measurements associated with the computational tree of the LDPC code rooted at section  $\ell$ . The (realized) scaling factors found in (21) are given by

$$\hat{\mathbf{s}}_\ell(\mathbf{r}) = \frac{\prod_{p \in N_0(v_\ell)} \boldsymbol{\mu}_{c_p \rightarrow v_\ell}}{\left\| \prod_{p \in N_0(v_\ell)} \boldsymbol{\mu}_{c_p \rightarrow v_\ell} \right\|_1}. \quad (27)$$

where  $N_0(v_\ell)$  denotes the neighborhood of  $v_\ell$  including the local observation and  $\boldsymbol{\mu}_{c_0 \rightarrow v_\ell} = \boldsymbol{\alpha}_\ell$ . We are ultimately interested in Jacobian entries of the form

$$\begin{aligned} \frac{\partial \hat{\mathbf{s}}_\ell(\mathbf{r}, g)}{\partial \mathbf{r}_j(h)} &= \frac{\partial}{\partial \mathbf{r}_j(h)} \frac{\prod_{p \in N_0(v_\ell)} \boldsymbol{\mu}_{c_p \rightarrow v_\ell}(g)}{\left\| \prod_{p \in N_0(v_\ell)} \boldsymbol{\mu}_{c_p \rightarrow v_\ell} \right\|_1} \\ &= \frac{\partial}{\partial \mathbf{r}_j(h)} \frac{\boldsymbol{\alpha}_\ell(g) \prod_{p \in N(v_\ell)} \boldsymbol{\mu}_{c_p \rightarrow v_\ell}(g)}{\sum_{k \in \mathbb{F}_q} \boldsymbol{\alpha}_\ell(k) \prod_{p \in N(v_\ell)} \boldsymbol{\mu}_{c_p \rightarrow v_\ell}(k)} \end{aligned} \quad (28)$$

for  $g, h \in \mathbb{F}_q$  and  $\ell, j \in [L]$ . We adopt a divide-and-conquer approach to identify and bound these derivatives. Specifically, we focus on the rooted tree obtained by taking the factor graph of the outer LDPC code, setting  $v_\ell$  as the root, and retaining only the nodes involved in the computation of  $\hat{\mathbf{s}}_\ell(\mathbf{r}, g)$ . Under Condition 6, this sub-graph must form a proper tree; Fig. 2 offers a notional diagram to illustrate the outcome of this process.

We seek to bound the magnitude of the derivatives in (28) based on the distance between  $v_\ell$  and  $v_j$  in this rooted tree. We begin with local observations.

**Proposition 9.** (Local Observations) *The partial derivatives of  $\boldsymbol{\alpha}_j$  with respect to  $\mathbf{r}_k(h)$  are given by*

$$\frac{\partial \boldsymbol{\alpha}_j}{\partial \mathbf{r}_k(h)} = \begin{cases} \frac{1}{\tau^2} \boldsymbol{\alpha}_j(h) (\mathbf{e}_h - \boldsymbol{\alpha}_j) & j = k \\ 0 & j \neq k \end{cases} \quad (29)$$

$\forall h \in \mathbb{F}_q$  and where  $\tau > 0$  is the standard deviation of the effective observation.

*Proof:* As defined in (8), the vector  $\boldsymbol{\alpha}_j$  is given by

$$\boldsymbol{\alpha}_j(g) = \frac{e^{\frac{\mathbf{r}_j(g)}{\tau^2}}}{\sum_{k \in \mathbb{F}_q} e^{\frac{\mathbf{r}_j(k)}{\tau^2}}} \quad \forall g \in \mathbb{F}_q.$$

When  $j \neq k$ , it immediately follows that  $\partial \boldsymbol{\alpha}_j / \partial \mathbf{r}_k(h) = 0$  as  $\boldsymbol{\alpha}_j$  does not depend on  $\mathbf{r}_k(h)$ . We thus consider the case where  $k = j$ . When  $g = h$ , we have that

$$\begin{aligned} \frac{\partial \boldsymbol{\alpha}_j(h)}{\partial \mathbf{r}_j(h)} &= \frac{1}{\tau^2} \frac{e^{\frac{\mathbf{r}_j(h)}{\tau^2}}}{\sum_{k \in \mathbb{F}_q} e^{\frac{\mathbf{r}_j(k)}{\tau^2}}} - \frac{1}{\tau^2} \frac{e^{\frac{\mathbf{r}_j(h)}{\tau^2}} e^{\frac{\mathbf{r}_j(h)}{\tau^2}}}{\left( \sum_{k \in \mathbb{F}_q} e^{\frac{\mathbf{r}_j(k)}{\tau^2}} \right)^2} \\ &= \frac{1}{\tau^2} \boldsymbol{\alpha}_j(h) (1 - \boldsymbol{\alpha}_j(h)). \end{aligned}$$

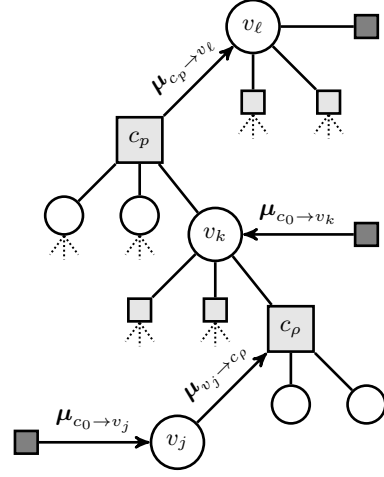


Fig. 2: Computation tree for variable node  $v_\ell$  obtained by taking the factor graph of the outer LDPC code, setting  $v_\ell$  as the root, and retaining only the nodes involved in the computation of  $\hat{\mathbf{s}}_\ell(\mathbf{r}, g)$ . We use this data structure to compute the derivatives in (28).

When  $g \neq h$ , we get

$$\frac{\partial \boldsymbol{\alpha}_j(g)}{\partial \mathbf{r}_j(h)} = -\frac{1}{\tau^2} \frac{e^{\frac{\mathbf{r}_j(g)}{\tau^2}} e^{\frac{\mathbf{r}_j(h)}{\tau^2}}}{\left( \sum_{\kappa \in \mathbb{F}_q} e^{\frac{\mathbf{r}_j(\kappa)}{\tau^2}} \right)^2} = -\frac{1}{\tau^2} \boldsymbol{\alpha}_j(g) \boldsymbol{\alpha}_j(h).$$

Collecting these findings and condensing them into a more compact form, we arrive at (29), which is the desired expression. ■

**Corollary 10.** *The absolute value of the partial derivatives of  $\boldsymbol{\alpha}_j$  with respect to  $\mathbf{r}_k(h)$  are bounded by*

$$\left| \frac{\partial \boldsymbol{\alpha}_j}{\partial \mathbf{r}_k(h)} \right| \leq \frac{1}{4\tau^2} \quad (30)$$

where  $\tau > 0$  is the standard deviation of the effective observation.

The proof of this corollary is trivial when  $\boldsymbol{\alpha}_j$  is a valid probability vector, as is the case in this article. We also note that, based on the state evolution of AMP,  $\tau^2 \geq \sigma^2$  at every iteration irrespective of the iteration number. We can therefore establish a uniform bound across iterations. We are now ready to show that the absolute value of (28) is bounded whenever  $\ell = j$ , i.e., at the root level of the computation tree.

**Proposition 11** (Root Derivatives). *The partial derivatives of  $\hat{\mathbf{s}}_\ell(\mathbf{r}, g)$  with respect to  $\mathbf{r}_\ell(h)$  are given by*

$$\frac{\partial \hat{\mathbf{s}}_\ell(\mathbf{r})}{\partial \mathbf{r}_\ell(h)} = \frac{1}{\tau^2} \hat{\mathbf{s}}_\ell(\mathbf{r}, h) (\mathbf{e}_h - \hat{\mathbf{s}}_\ell(\mathbf{r})) \quad \forall h \in \mathbb{F}_q \quad (31)$$

where  $\tau > 0$  is the standard deviation of the effective observation.



*Proof:* Leveraging Proposition 9 and denoting the standard inner product by  $\langle \cdot, \cdot \rangle$ , we have

$$\begin{aligned}
\frac{\partial \hat{\mathbf{s}}_\ell(\mathbf{r})}{\partial \mathbf{r}_\ell(h)} &= \frac{\partial}{\partial \mathbf{r}_\ell(h)} \frac{\boldsymbol{\alpha}_\ell \circ \bigcirc_{p \in N(v_\ell)} \boldsymbol{\mu}_{c_p \rightarrow v_\ell}}{\left\| \boldsymbol{\alpha}_\ell \circ \bigcirc_{p \in N(v_\ell)} \boldsymbol{\mu}_{c_p \rightarrow v_\ell} \right\|_1} \\
&= \frac{\boldsymbol{\alpha}_\ell(h) (\mathbf{e}_h - \boldsymbol{\alpha}_\ell) \circ \left( \bigcirc_{c_p \in N(v_\ell)} \boldsymbol{\mu}_{c_p \rightarrow v_\ell} \right)}{\tau^2 \left\| \boldsymbol{\alpha}_\ell \circ \left( \bigcirc_{c_p \in N(v_\ell)} \boldsymbol{\mu}_{c_p \rightarrow v_\ell} \right) \right\|_1} \\
&\quad - \frac{\boldsymbol{\alpha}_\ell(h)}{\tau^2} \hat{\mathbf{s}}_\ell(\mathbf{r}) \frac{\left\langle \mathbf{e}_h - \boldsymbol{\alpha}_\ell, \bigcirc_{c_p \in N(v_\ell)} \boldsymbol{\mu}_{c_p \rightarrow v_\ell} \right\rangle}{\left\| \boldsymbol{\alpha}_\ell \circ \left( \bigcirc_{c_p \in N(v_\ell)} \boldsymbol{\mu}_{c_p \rightarrow v_\ell} \right) \right\|_1} \\
&= \frac{\boldsymbol{\alpha}_\ell(h)}{\tau^2} \frac{\mathbf{e}_h \circ \left( \bigcirc_{c_p \in N(v_\ell)} \boldsymbol{\mu}_{c_p \rightarrow v_\ell} \right)}{\left\| \boldsymbol{\alpha}_\ell \circ \left( \bigcirc_{c_p \in N(v_\ell)} \boldsymbol{\mu}_{c_p \rightarrow v_\ell} \right) \right\|_1} \\
&\quad - \frac{\boldsymbol{\alpha}_\ell(h)}{\tau^2} \hat{\mathbf{s}}_\ell(\mathbf{r}) \frac{\left\langle \mathbf{e}_h, \bigcirc_{c_p \in N(v_\ell)} \boldsymbol{\mu}_{c_p \rightarrow v_\ell} \right\rangle}{\left\| \boldsymbol{\alpha}_\ell \circ \left( \bigcirc_{c_p \in N(v_\ell)} \boldsymbol{\mu}_{c_p \rightarrow v_\ell} \right) \right\|_1} \\
&= \frac{1}{\tau^2} \hat{\mathbf{s}}_\ell(\mathbf{r}, h) (\mathbf{e}_h - \hat{\mathbf{s}}_\ell(\mathbf{r})),
\end{aligned}$$

which is the desired expression.  $\blacksquare$

**Corollary 12.** *The absolute value of the partial derivatives of  $\hat{\mathbf{s}}_\ell(\mathbf{r})$  with respect to  $\mathbf{r}_\ell(h)$  are bounded by*

$$\left| \frac{\partial \hat{\mathbf{s}}_\ell(\mathbf{r})}{\partial \mathbf{r}_\ell(h)} \right| \leq \frac{1}{4\tau^2} \quad (32)$$

The proof of this corollary follows that of Corollary 10 because like  $\boldsymbol{\alpha}_j$ ,  $\hat{\mathbf{s}}_\ell(\mathbf{r})$  forms a valid probability vector.

Proposition 11 offers a blueprint for the general result we wish to establish. Yet, the situation gets more complicated when  $\ell \neq j$  because we have to involve the message passing rules. In doing so, we obtain a key intermediate result using mathematical induction. We start with the variable node closest to the root node, and then progress outward step by step.

To circumvent a notational nightmare, we restrict the proof to cases where all edge weights are equal to  $1 \in \mathbb{F}_q$ . Conceptually, the edge can be interpreted as permutations on the belief vectors. From the point of view of bounding partial derivatives, this is a benign operation, yet the accounting that comes with permutations is dreadful, hence our focus on the simpler case. Moving forward, we assume the following condition.

**Condition 13.** *All edge weights within the factor graph of the LDPC outer code are equal to  $1 \in \mathbb{F}_q$ .*

The extension of the following propositions to the case with arbitrary edge weights (i.e., beyond Condition 13) is conceptually straightforward.

**Proposition 14.** *Suppose Condition 6 holds and let  $v_j$  be a descendant of root node  $v_\ell$  in the computation tree. Moreover, let  $c_p \in N(v_\ell)$  be the unique check neighbor of  $v_\ell$  on the path from  $v_\ell$  to  $v_j$  within the tree. Then, there exists vector  $\boldsymbol{\nu}$ , with*

$\mathbf{0} \preceq \boldsymbol{\nu} \preceq \boldsymbol{\mu}_{c_p \rightarrow v_\ell}$ , such that the partial derivative of  $\boldsymbol{\mu}_{c_p \rightarrow v_\ell}$  with respect to  $\mathbf{r}_j(h)$  is given by

$$\frac{\partial \boldsymbol{\mu}_{c_p \rightarrow v_\ell}}{\partial \mathbf{r}_j(h)} = \frac{1}{\tau^2} \left( \boldsymbol{\nu} - \|\boldsymbol{\nu}\|_1 \boldsymbol{\mu}_{c_p \rightarrow v_\ell} \right), \quad (33)$$

where  $\tau > 0$  is the standard deviation of the effective observation. Here,  $\preceq$  denotes elementwise comparison of the entries in the vector.

*Proof:* Under condition 6, we know that  $v_j$  appears at most once within the computation tree rooted at  $v_\ell$ . Thus, we establish (33) via mathematical induction on the distance between  $v_\ell$  and its descendant  $v_j$  on the computation tree. The distance that we are interested in only considers the number of variable nodes between  $v_\ell$  and  $v_j$ . Before beginning, we point out that if  $v_j$  is not a descendant of  $v_\ell$ , then the corresponding partial derivatives vanish and the claim is immediate.

We begin with generic results that are useful for both the base case and the inductive step. Let  $v_j$  be a descendant of  $v_\ell$  and let  $v_k$  be the variable child of  $v_\ell$  on the path from  $v_\ell$  to  $v_j$ . Let  $c_p$  be the unique check node in  $N(v_\ell) \cap N(v_k)$  and let  $c_\rho$  be the unique check node child of  $v_k$  on the path from  $v_k$  to  $v_j$ ; if  $v_k = v_j$ , let  $\rho = 0$ . Then, we have that

$$\frac{\partial \boldsymbol{\mu}_{v_k \rightarrow c_p}}{\partial \mathbf{r}_j(h)} = \frac{\partial}{\partial \mathbf{r}_j(h)} \frac{\bigcirc_{c_\xi \in N_0(v_k) \setminus c_p} \boldsymbol{\mu}_{c_\xi \rightarrow v_k}}{\left\| \bigcirc_{c_\xi \in N_0(v_k) \setminus c_p} \boldsymbol{\mu}_{c_\xi \rightarrow v_k} \right\|_1}. \quad (34)$$

We can also examine the partial derivatives of the probability vector  $\boldsymbol{\mu}_{c_\rho \rightarrow v_k}$ . Suppose  $v_k \neq v_j$  and let  $v_o$  be the unique variable child of  $v_k$  on the path from  $v_\ell$  to  $v_j$ . Using the  $\mathbb{F}_q$  convolution, we have

$$\begin{aligned}
\frac{\partial \boldsymbol{\mu}_{c_\rho \rightarrow v_k}}{\partial \mathbf{r}_j(h)} &= \frac{\partial}{\partial \mathbf{r}_j(h)} \left( \bigcirc_{v_l \in N(c_\rho) \setminus v_k} \boldsymbol{\mu}_{v_l \rightarrow c_\rho} \right) \\
&= \frac{\partial \boldsymbol{\mu}_{v_o \rightarrow c_\rho}}{\partial \mathbf{r}_j(h)} \odot \left( \bigcirc_{v_l \in N(c_\rho) \setminus \{v_k, v_o\}} \boldsymbol{\mu}_{v_l \rightarrow c_\rho} \right) \\
&= \frac{\partial \boldsymbol{\mu}_{v_o \rightarrow c_\rho}}{\partial \mathbf{r}_j(h)} \odot \boldsymbol{\nu}_{c_\rho \setminus v_k, v_o}.
\end{aligned} \quad (35)$$

We emphasize that  $\boldsymbol{\nu}_{c_\rho \setminus v_k, v_o}$ , as defined implicitly above, is a probability distribution.

Having established these results, we turn our attention to the base case where  $v_j$  is a variable child of  $v_\ell$  ( $v_k = v_j$ ,

$\varrho = 0$ ). Applying (34) and Proposition 9, we obtain

$$\begin{aligned}
\frac{\partial \boldsymbol{\mu}_{v_j \rightarrow c_p}}{\partial \mathbf{r}_j(h)} &= \frac{\partial}{\partial \mathbf{r}_j(h)} \frac{\boldsymbol{\alpha}_j \circ \left( \bigcirc_{c_\xi \in N(v_j) \setminus c_p} \boldsymbol{\mu}_{c_\xi \rightarrow v_j} \right)}{\left\| \boldsymbol{\alpha}_j \circ \left( \bigcirc_{c_\xi \in N(v_j) \setminus c_p} \boldsymbol{\mu}_{c_\xi \rightarrow v_j} \right) \right\|_1} \\
&= \frac{\frac{\partial \boldsymbol{\alpha}_j}{\partial \mathbf{r}_j(h)} \circ \left( \bigcirc_{c_\xi \in N(v_j) \setminus c_p} \boldsymbol{\mu}_{c_\xi \rightarrow v_j} \right)}{\left\langle \boldsymbol{\alpha}_j, \bigcirc_{c_\xi \in N(v_j) \setminus c_p} \boldsymbol{\mu}_{c_\xi \rightarrow v_j} \right\rangle} \\
&\quad - \boldsymbol{\mu}_{v_j \rightarrow c_p} \frac{\left\langle \frac{\partial \boldsymbol{\alpha}_j}{\partial \mathbf{r}_j(h)}, \bigcirc_{c_\xi \in N(v_j) \setminus c_p} \boldsymbol{\mu}_{c_\xi \rightarrow v_j} \right\rangle}{\left\langle \boldsymbol{\alpha}_j, \bigcirc_{c_\xi \in N(v_j) \setminus c_p} \boldsymbol{\mu}_{c_\xi \rightarrow v_j} \right\rangle} \\
&= \frac{1}{\tau^2} \frac{\boldsymbol{\alpha}_j(h) \mathbf{e}_h \circ \left( \bigcirc_{c_\xi \in N(v_j) \setminus c_p} \boldsymbol{\mu}_{c_\xi \rightarrow v_j} \right)}{\left\langle \boldsymbol{\alpha}_j, \bigcirc_{c_\xi \in N(v_j) \setminus c_p} \boldsymbol{\mu}_{c_\xi \rightarrow v_j} \right\rangle} \\
&\quad - \frac{1}{\tau^2} \boldsymbol{\mu}_{v_j \rightarrow c_p} \frac{\left\langle \boldsymbol{\alpha}_j(h) \mathbf{e}_h, \bigcirc_{c_\xi \in N(v_j) \setminus c_p} \boldsymbol{\mu}_{c_\xi \rightarrow v_j} \right\rangle}{\left\langle \boldsymbol{\alpha}_j, \bigcirc_{c_\xi \in N(v_j) \setminus c_p} \boldsymbol{\mu}_{c_\xi \rightarrow v_j} \right\rangle} \\
&= \frac{1}{\tau^2} \left( \boldsymbol{\nu}_{v_j \rightarrow c_p} - \left\| \boldsymbol{\nu}_{v_j \rightarrow c_p} \right\|_1 \boldsymbol{\mu}_{v_j \rightarrow c_p} \right),
\end{aligned} \tag{36}$$

where

$$\boldsymbol{\nu}_{v_j \rightarrow c_p} = \frac{\boldsymbol{\alpha}_j(h) \mathbf{e}_h \circ \left( \bigcirc_{c_\xi \in N(v_j) \setminus c_p} \boldsymbol{\mu}_{c_\xi \rightarrow v_j} \right)}{\left\langle \boldsymbol{\alpha}_j, \bigcirc_{c_\xi \in N(v_j) \setminus c_p} \boldsymbol{\mu}_{c_\xi \rightarrow v_j} \right\rangle}.$$

By construction, we have  $\mathbf{0} \preceq \boldsymbol{\nu}_{v_j \rightarrow c_p} \preceq \boldsymbol{\mu}_{v_j \rightarrow c_p}$ . We turn to the second graph operation and apply (35), which yields

$$\begin{aligned}
\frac{\partial \boldsymbol{\mu}_{c_p \rightarrow v_\ell}}{\partial \mathbf{r}_j(h)} &= \frac{\partial \boldsymbol{\mu}_{v_j \rightarrow c_p}}{\partial \mathbf{r}_j(h)} \odot \boldsymbol{\nu}_{c_p \setminus v_\ell, v_j} \\
&= \frac{1}{\tau^2} \left( \boldsymbol{\nu}_{v_j \rightarrow c_p} - \left\| \boldsymbol{\nu}_{v_j \rightarrow c_p} \right\|_1 \boldsymbol{\mu}_{v_j \rightarrow c_p} \right) \odot \boldsymbol{\nu}_{c_p \setminus v_\ell, v_j} \\
&= \frac{1}{\tau^2} \left( \boldsymbol{\nu}_{v_j \rightarrow c_p} \odot \boldsymbol{\nu}_{c_p \setminus v_\ell, v_j} - \left\| \boldsymbol{\nu}_{v_j \rightarrow c_p} \right\|_1 \boldsymbol{\mu}_{c_p \rightarrow v_\ell} \right).
\end{aligned} \tag{37}$$

Thus, in this case, we take  $\boldsymbol{\nu} = \boldsymbol{\nu}_{v_j \rightarrow c_p} \odot \boldsymbol{\nu}_{c_p \setminus v_\ell, v_j}$  as a suitable vector. Based on the fact that  $\boldsymbol{\nu}_{c_p \setminus v_\ell, v_j}$  is a probability vector, together with the aforementioned component-wise ordering, we gather that

$$\begin{aligned}
\mathbf{0} &\preceq \boldsymbol{\nu} = \boldsymbol{\nu}_{v_j \rightarrow c_p} \odot \boldsymbol{\nu}_{c_p \setminus v_\ell, v_j} \\
&\preceq \boldsymbol{\mu}_{v_j \rightarrow c_p} \odot \boldsymbol{\nu}_{c_p \setminus v_\ell, v_j} = \boldsymbol{\mu}_{c_p \rightarrow v_\ell}.
\end{aligned}$$

Moreover, leveraging the properties of the  $\mathbb{F}_q$  convolution for non-negative vectors, we get

$$\left\| \boldsymbol{\nu} \right\|_1 = \left\| \boldsymbol{\nu}_{v_j \rightarrow c_p} \right\|_1 \left\| \boldsymbol{\nu}_{c_p \setminus v_\ell, v_j} \right\|_1 = \left\| \boldsymbol{\nu}_{v_j \rightarrow c_p} \right\|_1.$$

Thus, for this choice of  $\boldsymbol{\nu}$ , we arrive at

$$\frac{\partial \boldsymbol{\mu}_{c_p \rightarrow v_\ell}}{\partial \mathbf{r}_j(h)} = \frac{1}{\tau^2} \left( \boldsymbol{\nu} - \left\| \boldsymbol{\nu} \right\|_1 \boldsymbol{\mu}_{c_p \rightarrow v_\ell} \right), \tag{38}$$

as claimed. That is, the base case conforms to the structure of Proposition 14.

We now consider the inductive step in our proof. As our hypothesis, we assume that (33) holds for all computation trees wherein the distance between the root node and  $v_j$  is less than or equal to  $\gamma \in \mathbb{N}$ . Consider a rooted computation tree and

suppose the distance between  $v_\ell$  and its descendant  $v_j$  in the tree is exactly  $\gamma + 1$ . Under Condition 6, there is a unique path from  $v_\ell$  to node  $v_j$ . Let  $v_k$  be the variable child of  $v_\ell$  that is also an ascendant of  $v_j$ , and denote the unique check node that connects the two by  $c_p \in N(v_\ell) \cap N(v_k)$ . Furthermore, let  $c_\varrho \in N(v_k)$  be the unique check node within this neighborhood that is an ascendant of  $v_j$  on the computation tree. Finally, let  $v_o \in N(c_\varrho)$  be the unique variable child of  $v_k$  that is also an ascendant of  $v_j$  (or, perhaps,  $v_j$  itself).

The sub-tree starting at  $v_k$  can be viewed as a rooted tree containing  $v_j$ ; the graph distance between these two variable nodes within the sub-tree is exactly  $\gamma$ . As such, our inductive hypothesis applies. That is, there exists vector  $\boldsymbol{\nu}$  such that  $\mathbf{0} \preceq \boldsymbol{\nu} \preceq \boldsymbol{\mu}_{c_\varrho \rightarrow v_k}$  where the partial derivative of  $\boldsymbol{\mu}_{c_\varrho \rightarrow v_k}$  with respect to  $\mathbf{r}_j(h)$  is equal to

$$\frac{\partial \boldsymbol{\mu}_{c_\varrho \rightarrow v_k}}{\partial \mathbf{r}_j(h)} = \frac{1}{\tau^2} \left( \boldsymbol{\nu} - \left\| \boldsymbol{\nu} \right\|_1 \boldsymbol{\mu}_{c_\varrho \rightarrow v_k} \right). \tag{39}$$

Applying (34) and our inductive hypothesis, we have that

$$\begin{aligned}
\frac{\partial \boldsymbol{\mu}_{v_k \rightarrow c_p}}{\partial \mathbf{r}_j(h)} &= \frac{\partial}{\partial \mathbf{r}_j(h)} \frac{\bigcirc_{c_\xi \in N_0(v_k) \setminus c_p} \boldsymbol{\mu}_{c_\xi \rightarrow v_k}}{\left\| \bigcirc_{c_\xi \in N_0(v_k) \setminus c_p} \boldsymbol{\mu}_{c_\xi \rightarrow v_k} \right\|_1} \\
&= \frac{\frac{\partial \boldsymbol{\mu}_{c_\varrho \rightarrow v_k}}{\partial \mathbf{r}_j(h)} \circ \left( \bigcirc_{c_\xi \in N_0(v_k) \setminus c_p, c_\varrho} \boldsymbol{\mu}_{c_\xi \rightarrow v_k} \right)}{\left\langle \boldsymbol{\mu}_{c_\varrho \rightarrow v_k}, \bigcirc_{c_\xi \in N_0(v_k) \setminus c_p, c_\varrho} \boldsymbol{\mu}_{c_\xi \rightarrow v_k} \right\rangle} \\
&\quad - \boldsymbol{\mu}_{v_k \rightarrow c_p} \frac{\left\langle \frac{\partial \boldsymbol{\mu}_{c_\varrho \rightarrow v_k}}{\partial \mathbf{r}_j(h)}, \bigcirc_{c_\xi \in N_0(v_k) \setminus c_p, c_\varrho} \boldsymbol{\mu}_{c_\xi \rightarrow v_k} \right\rangle}{\left\langle \boldsymbol{\mu}_{c_\varrho \rightarrow v_k}, \bigcirc_{c_\xi \in N_0(v_k) \setminus c_p, c_\varrho} \boldsymbol{\mu}_{c_\xi \rightarrow v_k} \right\rangle} \\
&= \frac{1}{\tau^2} \frac{\boldsymbol{\nu} \circ \left( \bigcirc_{c_\xi \in N_0(v_k) \setminus c_p, c_\varrho} \boldsymbol{\mu}_{c_\xi \rightarrow v_k} \right)}{\left\langle \boldsymbol{\mu}_{c_\varrho \rightarrow v_k}, \bigcirc_{c_\xi \in N_0(v_k) \setminus c_p, c_\varrho} \boldsymbol{\mu}_{c_\xi \rightarrow v_k} \right\rangle} \\
&\quad - \frac{1}{\tau^2} \boldsymbol{\mu}_{v_k \rightarrow c_p} \frac{\left\langle \boldsymbol{\nu}, \bigcirc_{c_\xi \in N_0(v_k) \setminus c_p, c_\varrho} \boldsymbol{\mu}_{c_\xi \rightarrow v_k} \right\rangle}{\left\langle \boldsymbol{\mu}_{c_\varrho \rightarrow v_k}, \bigcirc_{c_\xi \in N_0(v_k) \setminus c_p, c_\varrho} \boldsymbol{\mu}_{c_\xi \rightarrow v_k} \right\rangle} \\
&= \frac{1}{\tau^2} \left( \boldsymbol{\nu}_{v_k \rightarrow c_p} - \left\| \boldsymbol{\nu}_{v_k \rightarrow c_p} \right\|_1 \boldsymbol{\mu}_{v_k \rightarrow c_p} \right),
\end{aligned} \tag{40}$$

where we have utilized the shorthand notation

$$\boldsymbol{\nu}_{v_k \rightarrow c_p} = \frac{\boldsymbol{\nu} \circ \left( \bigcirc_{c_\xi \in N_0(v_k) \setminus c_p, c_\varrho} \boldsymbol{\mu}_{c_\xi \rightarrow v_k} \right)}{\left\langle \boldsymbol{\mu}_{c_\varrho \rightarrow v_k}, \bigcirc_{c_\xi \in N_0(v_k) \setminus c_p, c_\varrho} \boldsymbol{\mu}_{c_\xi \rightarrow v_k} \right\rangle}.$$

We emphasize that two of the terms in the derivation above cancel out, as before. Furthermore, by construction, we immediately obtain  $\mathbf{0} \preceq \boldsymbol{\nu}_{v_k \rightarrow c_p} \preceq \boldsymbol{\mu}_{v_k \rightarrow c_p}$ . These observations closely parallel the description for the base case.

The derivation of the second graph operation for the inductive step is in complete analogy with the base case, except for labeling. Specifically, we apply (35) and obtain

$$\begin{aligned}
\frac{\partial \boldsymbol{\mu}_{c_p \rightarrow v_\ell}}{\partial \mathbf{r}_j(h)} &= \frac{\partial \boldsymbol{\mu}_{v_k \rightarrow c_p}}{\partial \mathbf{r}_j(h)} \odot \boldsymbol{\nu}_{c_p \setminus v_\ell, v_k} \\
&= \frac{1}{\tau^2} \left( \boldsymbol{\nu}_{v_k \rightarrow c_p} - \left\| \boldsymbol{\nu}_{v_k \rightarrow c_p} \right\|_1 \boldsymbol{\mu}_{v_k \rightarrow c_p} \right) \odot \boldsymbol{\nu}_{c_p \setminus v_\ell, v_k} \\
&= \frac{1}{\tau^2} \left( \boldsymbol{\nu}_{v_k \rightarrow c_p} \odot \boldsymbol{\nu}_{c_p \setminus v_\ell, v_k} - \left\| \boldsymbol{\nu}_{v_k \rightarrow c_p} \right\|_1 \boldsymbol{\mu}_{c_p \rightarrow v_\ell} \right).
\end{aligned} \tag{41}$$

For the inductive step, we define  $\boldsymbol{\nu}' = \boldsymbol{\nu}_{v_k \rightarrow c_p} \odot \boldsymbol{\nu}_{c_p \setminus v_\ell, v_k}$  as the candidate vector. Based on component-wise ordering, we can write

$$\begin{aligned} \mathbf{0} &\preceq \boldsymbol{\nu}' = \boldsymbol{\nu}_{v_k \rightarrow c_p} \odot \boldsymbol{\nu}_{c_p \setminus v_\ell, v_k} \\ &\preceq \boldsymbol{\mu}_{v_k \rightarrow c_p} \odot \boldsymbol{\nu}_{c_p \setminus v_\ell, v_k} = \boldsymbol{\mu}_{c_p \rightarrow v_\ell}. \end{aligned}$$

As before, we have that

$$\|\boldsymbol{\nu}'\|_1 = \|\boldsymbol{\nu}_{v_k \rightarrow c_p}\|_1 \|\boldsymbol{\nu}_{c_p \setminus v_\ell, v_k}\|_1 = \|\boldsymbol{\nu}_{v_k \rightarrow c_p}\|_1.$$

Hence, candidate vector  $\boldsymbol{\nu}'$  is such that  $\mathbf{0} \preceq \boldsymbol{\nu}' \preceq \boldsymbol{\mu}_{c_p \rightarrow v_\ell}$  and

$$\frac{\partial \boldsymbol{\mu}_{c_p \rightarrow v_\ell}}{\partial \mathbf{r}_j(h)} = \frac{1}{\tau^2} \left( \boldsymbol{\nu}' - \|\boldsymbol{\nu}'\|_1 \boldsymbol{\mu}_{c_p \rightarrow v_\ell} \right). \quad (42)$$

This completes the proof for Proposition 14.  $\blacksquare$

We have nearly attained our goal of showing that the magnitudes of the entries in the Jacobian matrix of  $\boldsymbol{\eta}(\mathbf{r})$  with respect to  $\mathbf{r}$  are uniformly bounded. To achieve the desired result, it suffices to connect the partial derivative of the incoming message with the partial derivative of state estimate  $\hat{\mathbf{s}}_\ell(\mathbf{r}, g)$ . This is accomplished below.

**Proposition 15.** *Under Condition 6, the absolute value of the entries in the Jacobian are bounded by*

$$\left| \frac{\partial \hat{\mathbf{s}}_\ell(\mathbf{r}, g)}{\partial \mathbf{r}_j(h)} \right| \leq \frac{1}{\tau^2} \quad \forall g, h \in \mathbb{F}_q, \ell, j \in [L], \quad (43)$$

where  $\tau > 0$  is the standard deviation of the effective observation.

*Proof:* When  $v_j$  does not appear in the rooted tree of  $v_\ell$ , the partial derivative is equal to zero and the result immediately follows. Furthermore, when  $v_\ell = v_j$ , the result follows from Corollary 12. Thus, we can focus on the scenario wherein  $v_j$  is a descendant of  $v_\ell$ .

Let  $c_p$  be the unique check node in  $N(v_\ell)$  that lies on the path between  $v_\ell$  and  $v_j$ . By Proposition 14, there exists vector  $\boldsymbol{\nu}$ , with  $\mathbf{0} \preceq \boldsymbol{\nu} \preceq \boldsymbol{\mu}_{c_p \rightarrow v_\ell}$ , such that the partial derivative of  $\boldsymbol{\mu}_{c_p \rightarrow v_\ell}$  with respect to  $\mathbf{r}_j(h)$  is given by

$$\frac{\partial \boldsymbol{\mu}_{c_p \rightarrow v_\ell}}{\partial \mathbf{r}_j(h)} = \frac{1}{\tau^2} \left( \boldsymbol{\nu} - \|\boldsymbol{\nu}\|_1 \boldsymbol{\mu}_{c_p \rightarrow v_\ell} \right). \quad (44)$$

Drawing an analogy to (40), we have

$$\begin{aligned} \frac{\partial \hat{\mathbf{s}}_\ell(\mathbf{r})}{\partial \mathbf{r}_j(h)} &= \frac{\partial}{\partial \mathbf{r}_j(h)} \frac{\bigcirc_{c_\xi \in N_0(v_\ell)} \boldsymbol{\mu}_{c_\xi \rightarrow v_\ell}}{\left\| \bigcirc_{c_\xi \in N_0(v_\ell)} \boldsymbol{\mu}_{c_\xi \rightarrow v_\ell} \right\|_1} \\ &= \frac{1}{\tau^2} \frac{\boldsymbol{\nu} \circ \left( \bigcirc_{c_\xi \in N_0(v_\ell) \setminus c_p} \boldsymbol{\mu}_{c_\xi \rightarrow v_\ell} \right)}{\left\langle \boldsymbol{\mu}_{c_p \rightarrow v_\ell}, \bigcirc_{c_\xi \in N_0(v_\ell) \setminus c_p} \boldsymbol{\mu}_{c_\xi \rightarrow v_\ell} \right\rangle} \\ &\quad - \frac{1}{\tau^2} \hat{\mathbf{s}}_\ell(\mathbf{r}) \frac{\left\langle \boldsymbol{\nu}, \bigcirc_{c_\xi \in N_0(v_\ell) \setminus c_p} \boldsymbol{\mu}_{c_\xi \rightarrow v_\ell} \right\rangle}{\left\langle \boldsymbol{\mu}_{c_p \rightarrow v_\ell}, \bigcirc_{c_\xi \in N_0(v_\ell) \setminus c_p} \boldsymbol{\mu}_{c_\xi \rightarrow v_\ell} \right\rangle} \\ &= \frac{1}{\tau^2} \left( \boldsymbol{\nu}_{v_\ell} - \|\boldsymbol{\nu}_{v_\ell}\|_1 \hat{\mathbf{s}}_\ell(\mathbf{r}) \right), \end{aligned} \quad (45)$$

where we have implicitly defined

$$\boldsymbol{\nu}_{v_\ell} = \frac{\boldsymbol{\nu} \circ \left( \bigcirc_{c_\xi \in N_0(v_\ell) \setminus c_p} \boldsymbol{\mu}_{c_\xi \rightarrow v_\ell} \right)}{\left\langle \boldsymbol{\mu}_{c_p \rightarrow v_\ell}, \bigcirc_{c_\xi \in N_0(v_\ell) \setminus c_p} \boldsymbol{\mu}_{c_\xi \rightarrow v_\ell} \right\rangle}.$$

We note that  $\mathbf{0} \preceq \boldsymbol{\nu}_{v_\ell} \preceq \hat{\mathbf{s}}_\ell(\mathbf{r})$ . Thus, we have that:

$$\frac{\partial \hat{\mathbf{s}}_\ell(\mathbf{r})}{\partial \mathbf{r}_j(h)} \leq \frac{1}{\tau^2} \boldsymbol{\nu}_{v_\ell} \leq \frac{1}{\tau^2} \hat{\mathbf{s}}_\ell(\mathbf{r}). \quad (46)$$

Since we are interested in bounding the absolute value of the partial derivatives, we also consider a lower bound.

$$\frac{\partial \hat{\mathbf{s}}_\ell(\mathbf{r})}{\partial \mathbf{r}_j(h)} \geq -\frac{1}{\tau^2} \|\boldsymbol{\nu}_{v_\ell}\|_1 \hat{\mathbf{s}}_\ell(\mathbf{r}) \geq -\frac{1}{\tau^2} \hat{\mathbf{s}}_\ell(\mathbf{r}). \quad (47)$$

Combining these two observations with the properties of probability vectors, we obtain the desired expression.  $\blacksquare$

**Theorem 16.** *Under Condition 6, the BP-N denoiser presented in definition 5 is Lipschitz continuous.*

*Proof:* By Proposition 15, the magnitudes of the entries of the Jacobian matrix of  $\boldsymbol{\eta}(\mathbf{r})$  with respect to  $\mathbf{r}$  are uniformly bounded. Thus, the denoiser is Lipschitz continuous.  $\blacksquare$